Acta Geologica Sinica (English Edition), 2022, 96(4): 1388–1401

1922—2022

Evaluation Methods and Indexes for Ultra-deep Petroleum Reservoir Preservation with Case Studies

YUAN Yusong[1, *], WANG Guojian[1], HU Wenxuan[2], CHEN Shuping[3], WANG Xiaolin[2], ZOU Yu[1], WANG Xinpeng[3], ZHANG Rongqiang[1] and HAO Yunqing[1]

[1] *Research Institute of Petroleum Exploration and Development, Sinopec, Beijing 100038, China*
[2] *School of Earth Science and Engineering, Nanjing University, Nanjing 210008, China*
[3] *School of Geosciences, Chinese University of Petroleum (Beijing), Beijing 102200, China*

Abstract: Following consideration of the characteristics of high temperature, high pressure and high in-situ stress in ultra-deep sedimentary basins, together with the existence of hydrocarbon phase state transformation, hydrocarbon-water-rock interaction and rock mechanical property transition at those depths, the evaluation index system for hydrocarbon preservation was established. The physical leakage evaluation indexes can be divided into three categories: the dynamic efficiency indexes of micro-sealing, caprock integrity and natural gas diffusion. The chemical loss evaluation indexes can be divided into two categories: the thermochemical sulfate reduction (TSR) index in marine gypsum-bearing carbonate strata and the thermochemical oxidation of hydrocarbons (TOH) index in clastic strata. The slippage angle and overconsolidation ratio (OCR) are the key evaluation indexes in the evaluation of the integrity of shale caprocks. TSR intensity can be quantitatively calculated by use of the ZnPVT state parameter method. The TOH strength can be used to estimate the degree of hydrocarbon chemical loss, based on the TOH-related authigenic calcite cement content or the degree of negative $\delta^{13}C$ of authigenic calcite. For the evaluation of ultra-deep preservation in specific areas, key indexes can be selected according to the local geological conditions, instead of all indexes needing to be evaluated for every scenario.

Key words: ultra-deep, hydrocarbon preservation, physical leakage, chemical loss, thermochemical sulfate reduction, thermochemical oxidation of hydrocarbons

Citation: Yuan et al., 2022. Evaluation Methods and Indexes for Ultra-deep Petroleum Reservoir Preservation with Case Studies. Acta Geologica Sinica (English Edition), 96(4): 1388–1401. DOI: 10.1111/1755-6724.14969

1 Introduction

In the course of the development of oil and gas exploration, geologists have come to realize that, with regard to the process of petroleum accumulation and reservoir formation, 'hydrocarbon generation' is the basis and 'preservation' is the key (Li et al., 1997). Petroliferous basins located in active tectonic zones, or those transformed by multiple tectonic events, need superior caprocks (Jin, 2012). Natural gas has molecular diameters that are smaller than oil, making it comparatively easy for it to diffuse and permeate, imposing more stringent restrictions on the caprocks (Dai, 2003). Destruction styles of marine hydrocarbon reservoirs mainly include the cutting of faults, uplifting and erosion, fold alteration, deep-burial cracking, baking of magma, fluid washing, biodegradation, long-term diffusion etc. (He et al., 2017). In terms of risk, three physical leakage means by which the caprock of petroleum reservoirs can fail have been identified: diffusive loss through the caprock, leakage through pore spaces when capillary breakthrough pressure has been exceeded and leakage through faults or fractures. In addition, any of these processes can occur in combination with others (Song and Zhang, 2013). The evaluation technology system of oil and gas preservation conditions of marine strata in southern China was established based on five aspects: the caprock and its sealing performance, fault sealing, late tectonic intensity, hydrogeological conditions and the subsurface hydrolyzation characteristics of mechanical-dynamic behavior (Ma et al., 2006).

Prior studies on petroleum preservation generally did not emphasize ultra-deep (>6500 m) geological settings, which are characterized by high temperatures, high pressures and high in-situ stresses. Ultra-deep caprocks are characterized by intense compaction, deep diagenetic evolution, low porosity, low permeability, high displacement pressure and therefore possess excellent micro-sealing ability. Moreover, ultra-deep reservoirs usually have a multi-stage sealing system composed of regional and local caprocks, where the oil and gas preservation conditions are generally also excellent. However, this does not mean that there is no need to pay attention to hydrocarbon preservation evaluation in ultra-deep oil and gas exploration, because the geological environment provides conditions for phase state transformation of hydrocarbons (Zhao et al., 2001), hydrocarbon-water-rock interaction (Ma and Zhao, 2016; Hu et al., 2018) and rock mechanical properties transition (Rybacki et al., 2016). Thus, it has been determined that

* Corresponding author. E-mail: yuanys.syky@sinopec.com

http://www.geojournals.cn/dzxbcn/ch/index.aspx; https://onlinelibrary.wiley.com/journal/17556724

the mode of destruction of ultra-deep oil and gas reservoirs may be either through physical leakage or chemical loss, or both (Yuan et al., 2019).

Physical leakage includes Darcy flow, which is dominated by faults and overpressure ruptures, micro-leakage, dominated by micro-cracks and connected pores, as well as gas diffusion caused by gas concentration differences. The chemical loss of hydrocarbons is mainly a product of phase transformation of hydrocarbons (such as oil cracking) dominated by high temperature and high pressure, thermochemical sulfate reduction (TSR) (Cai et al., 2013) and thermochemical oxidation of hydrocarbons (TOH) (Hu et al., 2018) caused by redox reactions. Therefore, the basic idea of evaluating ultra-deep oil and gas preservation conditions should be conducted from two perspectives: physical leakage and chemical loss (Yuan et al., 2019). Based on the main controlling factors of physical leakage and chemical loss of ultra-deep hydrocarbons, the evaluation index system of ultra-deep hydrocarbon preservation conditions is clarified, with the technical methods for determination of the key indexes being established.

2 Main Controlling Factors of Hydrocarbon Preservation in the Ultra-deep Reservior

Ultra-deep hydrocarbon preservation is primarily affected by physical leakage and chemical losses (Fig. 1). There are three modes of physical hydrocarbon leakage in reservoirs: Darcy flow, microleakage and diffusion. Darcy flow is mainly affected by caprock integrity, which is controlled by faults and fractures in the caprocks, micro-leakage occurring to overcome caprock capillaries and diffusion is almost everywhere, for as long as there is a difference in hydrocarbon concentration, there will be diffusion of hydrocarbons. There are thermochemical sulfate reduction (TSR) and thermochemical oxidation of hydrocarbons (TOH) types of hydrocarbon chemical losses in reservoirs, which are both strictly constrained by temperature (Yuan et al., 2019).

2.1 Controlling factors of hydrocarbon physical leakage

2.1.1 Integrity of caprocks

(1) Faulting

Faults are one of the important factors affecting the leakage of hydrocarbons in Darcy flow. The sealing behavior of faults in active and inactive phases is quite different. They are usually unsealed during the active stage and only in the inactive stage is it possible to seal oil and gas (Færseth et al., 2007). Therefore, when evaluating the fault sealing of a specific area, it must be related to regional tectonic events, the development and activity time of the fault must first be determined. There are two main types of fault sealing indexes in the inactive stage: lithology juxtaposition sealing and fault rock sealing (Faulkner et al., 2010). A lithological juxtaposition diagram of the upper/footwall of a fault (Allan diagram) is often used to evaluate fault sealing (Allan, 1989). For shale with low diagenetic evolution, mudstone/shale smear potential, mudstone/shale gouge ratio and mudstone fault ratio are all important parameters for evaluating fault sealing (Weber et al., 1978). Stress history plays an important role in controlling the sealing property of faults, especially faults with gouge. In a shear fault zone, the mechanical properties of mudstone or shale are closely related to fault sealing. When shear failure occurs in normally consolidated mudstone with ductile characteristics, permeability decreases. When shear failure occurs in overconsolidated mudstone with brittle characteristics, permeability increases (Bolton et al., 1998). When the local stress reaches 25 MPa and the shear strain reaches 10, the permeability can be reduced by 2–3 orders of magnitude, even in the fault zone without gouge development (Zhang and Tullis, 1998). In addition to fault sealing, fault-caprock configuration is also one of the important factors affecting fault sealing. When high-quality salt caprocks exist, oil and gas can still be well preserved, even in imbricate structures where faults are extremely well-developed, such as the Kelasu Gas Field in the Kuqa Depression (Wang et al., 2016).

Under ultra-deep conditions, the increase in confining

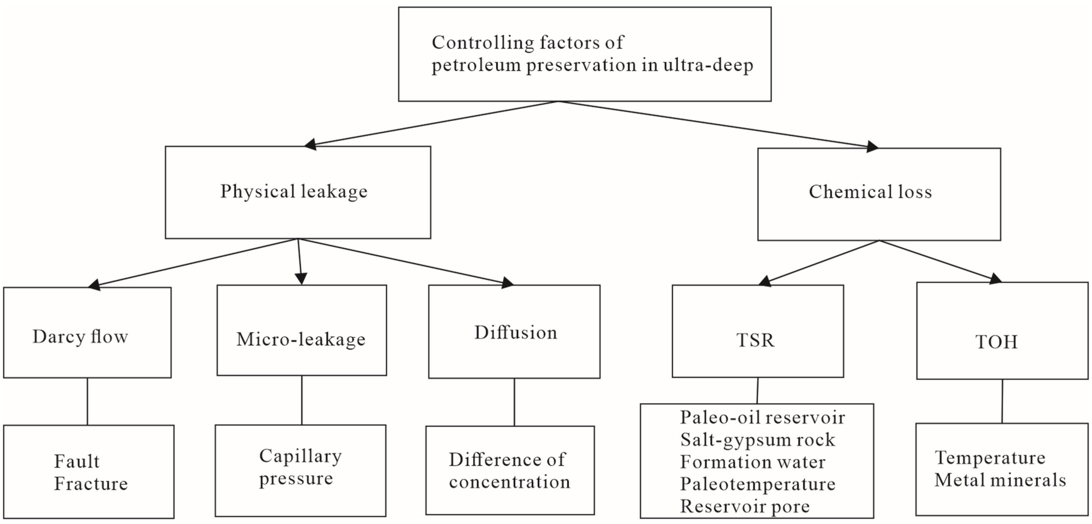

Fig. 1. Chart showing the controlling factors for hydrocarbon preservation in the ultra-deep environment.

pressure leads to the decrease of rock brittleness and increase of ductility, enhancing fault sealing, especially in the mudstone or shale segment. Therefore, the sealing evaluation of ultra-deep faults needs to include mechanical parameters that reflect the brittleness and ductility of rocks, such as the overconsolidation ratio (OCR). It is feasible, both theoretically and technically, to evaluate the sealing ability of an ultra-deep non-active period, by combining the fault sealing index and the OCR.

(2) Fractures in caprocks

Caprock fracture is another factor affecting the dispersion of hydrocarbons in Darcy flow. The development, nature and healing degree of fractures directly affect the integrity of caprocks (Chitrala et al., 2013). The fractures related to the sealing property of caprock are mainly tectonic fractures. Non-tectonic fractures generally have little impact on the preservation of oil and gas (Yuan et al., 2015). In addition, the overpressure fracture caused by uplift is also one of the important factors. Along with tectonic stress, the slip angle of the bedding and the mechanical properties of the rocks are the key factors controlling the formation and evolution of fractures, including fracture properties and the degree of fracture healing. Once cracks occur, the integrity of the caprocks will be destroyed. However, in the ultra-deep environment, the overlying strata are very thick, the fractures becoming closed under the overlying lithostatic stress. The degree of fracture healing is the key factor affecting the sealing property of the caprocks, which controls the degree of restoration of the integrity of the caprocks (Larsen and Gudmundsson, 2010). Therefore, the combination of fracture healing depth and OCR can be used to evaluate whether and to what extent the fracture-related caprock integrity has been repaired.

2.1.2 Dynamic microscopic sealing effectiveness of caprocks

Caprock capillary pressure (displacement pressure) controls the microscopic sealing capacity of caprocks and is the most effective evaluation parameter (Lv et al., 1993). The matrix porosity and permeability of the caprocks that have experienced an ultra-deep burial depth must be very low and the microscopic sealing must be excellent, for the integrity of the caprocks not to be destroyed. For ultra-deep caprocks, the main problem is not micro-sealing, but the effectiveness of the sealing, which is the match in the relationship between the seal formation time and the timing of kerogen hydrocarbon generation or oil cracking to gas. Only when the seal formation time of caprocks is earlier than the time of hydrocarbon generation by source rocks and oil cracking to gas, or at least no later than the main gas generation period of source rocks and the end point of oil cracking to gas, with the sealing property of the caprocks having been maintained since its formation, is it an effective caprock (Yuan et al., 2011).

2.1.3 Natural gas diffusion

The diffusion of natural gas is due to molecular movement. The difference in hydrocarbon concentration is the driving force for the diffusion and migration of natural gas molecules. The diffusive behavior of natural gas primarily occurs in rock pores with very low permeability. Such diffusion is limited by pore size, shape, degree of bending and even lithological characteristics, as well as being affected by temperature and pressure (Fu and Su, 2004). Diffusion is different from leakage, in that it does not require a pressure difference, but only a concentration difference. To sum up studies on the diffusion mechanism, of natural gas (Kim et al., 2016; Chen et al., 2018), it is generally believed that the diffusion mechanisms of natural gas generally include: 1) Fick diffusion, usually occurring in large pores and under high pressure, that is, collisions between gas molecules are more obvious than those between gas molecules and pore walls; 2) Knudsen diffusion, where the average free path of gas molecules is larger than the pore size, the collision between gas molecules and the pore wall being more obvious, this diffusion mode playing a dominant role in shale gas transportation; 3) surface diffusion, the driving force of which is the chemical potential gradient. For strongly adsorbent or nano pores, surface diffusion is significant. In addition, it is believed that methane gas molecules also engage in a form of dissolved gas diffusion in porous media (Chen et al., 2018). After adsorbed gas is desorbed from the pore wall of organic matter, there is a concentration gradient of dissolved gas in the organic matter, which is the driving force of dissolved gas diffusion.

The main controlling factors of the natural gas diffusion coefficient include: 1) physico-chemical properties of the diffuser, such as molar mass, molecular size, geometric shape, molecular polarity and solubility; 2) the properties of the diffusion medium, such as porosity, pore structure (pore diameter, curvature, connectivity), pore fluid composition (viscosity, polarity, ionic strength, solubility), mineral organic matter composition (mineral adsorption, specific surface area); 3) boundary conditions: pore pressure, temperature and initial concentration (Krooss et al., 1985, 1988). Although there are many experimental studies on the diffusion coefficient of natural gas in rock, none of them can simulate the real primary controlling factors. In the laboratory diffusion coefficient determination process, the setting of temperature and pressure conditions is generally lower than on the actual scenario of ultra-deep formation, the multi-scale pore structure of the rock and the supercritical conditions caused by high pressures and high temperatures are not fully considered, while the coefficient correction is mostly carried out in saturated media temperature and pressure conditions (Taghavinejad et al., 2020; Jing et al., 2021). These results cannot reflect the authenticity of approximating ultra-deep formation conditions. Therefore, a satisfactory test instrument is critical in order to obtain a reliable diffusion coefficient under the conditions of multi-stage sealing at ultra-deep high temperatures and pressures.

2.2 Controlling factors of hydrocarbon chemical loss

There are two main types of chemical loss of ultra-deep hydrocarbons. One is thermochemical sulfate reduction (TSR) in ultra-deep marine gypsum-bearing carbonate rocks. TSR is a chemical reaction in which sulfate minerals are reduced to sulfide by hydrocarbons under thermal dynamic drive while hydrocarbons are oxidized to acidic gases such as H_2S and CO_2. It is a geological-geochemical process of organic-inorganic fluid interaction prevalent in oil and gas reservoirs with gypsum carbonate reservoirs at high temperature (Cai and Li, 2005). Ultra-deep (>6500 m) usually meets the high temperature conditions required by TSR (under formation conditions, >120° C). When TSR occurs, it causes hydrocarbon consumption. The other form of chemical loss is the thermal oxidation of hydrocarbons (TOH) by high-valence metal oxides in ultra-deep clastic formations, such as Fe^{3+} and Mn^{4+}, which can oxidize methane and other hydrocarbons to CO_2 under certain temperature conditions, thus consuming hydrocarbons (Hu et al., 2018).

2.2.1 Main controlling factors of TSR

In the marine carbonate strata of southern China, TSR on a certain scale usually meets five conditions simultaneously (Yuan et al., 2021): 1) existence of paleo-oil reservoirs; 2) thin sequences of paste rock; 3) adequate formation water; 4) subjected to palaeotemperatures higher than 120°C; 5) the reservoir is porous dolomite. The paleo-oil reservoirs provide abundant C^{2+} rich hydrocarbons prone to TSR; thin sequences of paste rock and formation water together provide a sulfate-rich solution; high temperature provides heat; the porous dolomite reservoir provides accommodation for hydrocarbon-water-rock interaction.

The paleo-oil reservoir provides sufficient hydrocarbon (reactants) for TSR, which is an important controlling factor for the formation of gas reservoirs with high H_2S content. All the reservoirs with high H_2S content in the Sichuan Basin have paleo-oil reservoirs. In contrast, the H_2S content in the reservoirs without paleo-oil reservoirs is not high. In theory, organic matter, as an important reducing agent, can be either hydrocarbon in oil and gas reservoirs or dispersed soluble and insoluble organic matter (kerogen). Even if TSR occurs in dispersed soluble and insoluble organic matter (kerogen), the products are likely to be dispersed and not necessarily aggregated into reservoirs. H_2S is much more chemically active than CH_4 in the process of accumulation, if it does accumulate. TSR occurs in ancient reservoirs in-situ and forms natural gas reservoirs, the generated H_2S being easier to preserve and detect (Cai and Li, 2005). Therefore, under actual geological conditions, high H_2S gas reservoirs are often associated with ancient oil reservoirs.

Gypsum provides a sulfur source for TSR, sulfate (gypsum) in carbonate-evaporite profiles providing the basic material for H_2S formation. All gas fields with high H_2S content in the Sichuan Basin are directly or indirectly related to the distribution of gypsum in marine carbonate-evaporite profiles. In actual geological scenarios, gypsum is the most important source of sulfate solutions, the development and distribution of gypsum rock being one of the main controlling factors of TSR.

The formation water dissolves the gypsum rock and provides sulfate for TSR. TSR is a reaction between sulfate radicals and water-soluble organic matter. Solid sulfate only directly reacts with hydrocarbons with difficulty. Chemically, TSR requires a sulfate solution rather than the gypsum itself, which is one of the reasons why there is no correlation between TSR strength and gypsum thickness (Cai et al., 2017).

The initial temperature of TSR under geological conditions is approximately 120–140° C (Cai and Li, 2005). Under the same geological conditions, the temperature is positively correlated with H_2S content within a specific temperature range. The greater the burial depth (and therefore the higher the temperature) of the Feixianguan Formation gas reservoir in the Sichuan Basin, the higher the H_2S content (Zhu et al., 2014).

TSR usually occurs in carbonate rocks rather than clastic rocks, being dominated by porous dolomite reservoirs rather than fractured or tight limestone. The gypsum rocks that provide TSR's reactants (sulfate) are usually symbiotic with carbonate formations, the pore type reservoir providing the initial accommodation space for the hydrocarbon-water-rock interaction, TSR also further transforming the pore space of the dolomite reservoir.

2.2.2 Main controlling factors of TOH

The main controlling factors of TOH are the formation temperature and the content of high valence metal minerals. The oxidation of CH_4, induced by the chloritization of detrital ferriferous biotite at approximately 270° C in the Swiss Alps, led to the transition of the fluids from a methane/water zone into a water/CO_2 zone (Tarantola et al., 2007). The thermochemical oxidation of methane, $C_{13}H_{28}$ and alcohol compounds (here CH_3OH and C_2H_5OH) by MnO_2 can proceed efficiently at temperatures below 200°C and CH_4 can be oxidized by Fe_2O_3 at a temperature not lower than 250°C as determined by Raman spectroscopy combined with fused silica capillary capsules (Wan et al., 2021). Examples of geological case studies implied that the thermochemical oxidation of organic components can steadily occur at relatively lower temperatures. For example, thermochemical oxidation of hydrocarbons by high valence state manganese species occurred between 90 and 135°C (Hu et al., 2018) in the Junggar Basin (NW China), on the basis of detailed carbon isotopic analyses of authigenic calcite combined with measurements of the fluid inclusions. According to TSR and hydrocarbon generation reaction temperatures of organic matter in source rocks under geological conditions and TOH of the Baikouquan Formation in the Junggar Basin, CH_4 can be oxidized by high-valence Mn to form CO_2 at 110ºC under actual geological conditions (Hu et al., 2018). The higher the content of high-valence metal oxides (MnO_2, Fe_2O_3) in the reservoir, the greater the chemical loss of TOH hydrocarbons.

3 Evaluation Indexes and Determination Methods for Ultra-deep Hydrocarbon Preservation

The evaluation of ultra-deep oil and gas preservation conditions needs to be studied from the perspectives of both physical leakage and chemical loss (Yuan et al., 2019), so the evaluation index system includes both the physical leakage evaluation index and the chemical loss evaluation index.

3.1 Physical leakage evaluation indexes and determination methods

3.1.1 Physical leakage evaluation indexes

The basic ideas underlying the establishment of the ultra-deep physical leakage evaluation index system, are that: 1) brittle shale tends to produce tensile fractures, resulting in loss of integrity of caprocks; 2) shale has the characteristics of brittle-ductile transformation and, when the confining pressure is high enough, brittle-ductile transformation will occur (Gueydan et al., 2001; Dehandschutter et al., 2004; Nankali, 2012; Yuan et al., 2017); 3) ductile shale is not easy to produce tensile fractures in and plastic deformation tends to occur under tectonism, which is conducive to maintaining the integrity of caprocks; 4) overpressure rupture of organic-rich shale with a high degree of evolution may occur during uplift, resulting in loss of integrity of caprocks (Cobbold et al., 2013); 5) when the tectonic stress that caused the fracture is released, fracture healing occurs under deep burial conditions, but the degree of fracture healing is affected by OCR; 6) the smaller the OCR, the greater the ductility of the shale (Nygard et al., 2006), the higher the healing degree of fracture by the overburden, the more easily the caprock integrity can be reconstructed, but, in contrast, the larger the OCR, the greater the brittleness, the lower the healing degree of fracture, the lower the degree of repair of caprock integrity, the more serious the damage to preservation conditions is; 7) in the circumstance where the integrity of the caprock is intact, the dynamic validity of the caprock becomes the key index, so that the evaluation index of the dynamic matching relationship between the source and the caprock is included to determine the dynamic validity of the microscopic sealing within its geological history (Yuan et al., 2010); 8) in order to make clear the influence of gas diffusion on the sustaining time of oil and gas reservoirs under ultra-deep conditions, gas diffusion is considered when the integrity of the caprock is good and the micro-sealing is dynamically effective.

According to the above basic concepts, the physical leakage evaluation indexes of ultra-deep oil and gas preservation can be divided into three categories: first, the dynamic efficiency indexes of caprock micro-sealing, second, the evaluation index of caprock integrity and third is the evaluation index of gas diffusion.

The dynamic effectiveness index of the micro-seals is mainly the dynamic matching relationship of the source/caprock, which can be divided into three categories, namely full matching of source/caprock, partial matching of source/caprock and mismatching of source/caprock. In other words, the sealing formation time of the caprock is earlier than the hydrocarbon generation time of the source rocks and the cracking time of the paleo-oil reservoir, the caprock sealing ability having been maintained until now. Partial source/caprock matching means that the sealing formation time of the caprock is no later than the end time of hydrocarbon generation of the source rocks and the oil cracking time of the paleo-oil reservoir, the sealing ability having been maintained until now. Source/caprock mismatch means that the sealing formation time of the caprock is later than the hydrocarbon generation time of the source rocks and the end time of oil cracking into gas.

The evaluation indexes of caprock integrity include those related to faults and cracks in caprocks. In the ultra-deep environment, the fault sealing index (I) and the overconsolidation ratio (OCR) can be considered as the evaluation indexes of the integrity of the caprock as related to faults. When the sealing index is greater than 1 (that is, the normal stress on the fault is greater than the formation pressure) and the OCR value is quite small, the fault is closed and the preservation conditions are not damaged. Otherwise, the fault acts against preservation. There are six evaluation indexes related to caprock integrity relating to fracture: 1) bedding slippage angle (θ) of shale caprock: when bedding slippage angle equals to 45 minus half of internal friction angle of shale it is easy to produce bedding slippage fracture and therefore damage integrity; 2) overpressure rupture coefficient (f): when the formation fluid pressure coefficient is greater than the overpressure rupture coefficient of the caprock, the caprock is broken and therefore the integrity is destroyed; 3) bottom boundary of brittle zone (Z_b): when the burial depth of shale caprock is above the bottom boundary of the brittle zone, brittle cracks are likely to occur; 4) top boundary of ductility zone (Z_d): when the burial depth of shale caprock is closer or below the top boundary of the ductility zone, brittle cracks are not likely to occur in the caprock, the integrity being good; 5) the fracture healing depth (Z_c): when the burial depth of the caprock is below the healing depth, fracture healing occurs and therefore the integrity to some extent being repaired; 6) overconsolidation ratio (OCR): the degree of fracture healing is related to OCR, the smaller the OCR is, the higher the degree of fracture healing, the better the degree of caprock integrity repair is.

The evaluation indexes related to natural gas diffusion are mainly the diffusion coefficient (D) of natural gas under ultra-deep temperature and pressure conditions and multi-stage sealing caprocks. The higher the diffusion coefficient is, the faster the gas diffusion loss.

3.1.2 Determination methods for physical leakage evaluation indexes

The determination method of the dynamic effectiveness of microscopic sealing of caprocks is detailed in the literature (Yuan et al., 2010, 2011; Jin et al., 2014), so will not be elaborated on here. This study only introduces the methods of determining the index of caprock integrity and the index of diffusion coefficient under subsurface conditions.

(1) Bedding slippage angle of shale caprocks (θ) (Lu, 2010)

$$\theta = 45 - \phi/2 \tag{1}$$

where ϕ is the internal friction angle of the shale, in degrees.

As the internal friction angles of different types of shale are different, the bedding slippage angles of different shale caprocks are also different. The internal friction angle of shale can be obtained using the triaxial compression test. Samples for triaxial compression testing were obtained from the Silurian Longmaxi shale in the Jiaoshiba area of the Sichuan Basin. Methods of triaxial compression test were introduced in some previous work (Amann et al., 2012; Tarasov and Potvin, 2013). The results show that the internal friction angle is about 30° (Table 1; Yuan et al., 2020).

When the angle between the maximum principal stress and the bedding (bedding slippage angle) is θ = 45° − 30°/2 = 30°, bedding shear is likely to occur, resulting in bedding slippage cracks. However, the Silurian Longmaxi Formation of well JY–1 has a dip angle of 5°–10°. The included angle between the bedding plane of the shale and horizontal stress is very small, which differs greatly from the bedding slippage angle. Therefore, shear failure is unlikely to occur, the integrity of caprock being well-maintained in well JY–1.

(2) Overpressure rupture coefficient (*f*)

$$f = 2.0 + 0.5 K_h \qquad (2)$$

where f is the overpressure rupture coefficient of shale, dimensionless; K_h, additional tectonic stress coefficient along the direction of minimum horizontal principal stress; dimensionless. Thus, the conditions for overpressure fracture of shale are as follows:

$$P_f = (2.0 + 0.5 K_h)\rho_w gZ \qquad (3)$$

where P_f is the formation fluid pressure, MPa; ρ_w, formation water density, g/cm^3; G, acceleration of gravity, m/s^2; Z, depth, m. The additional tectonic stress coefficient (K_h) along the direction of minimum horizontal principal stress can be obtained from drilling hydraulic fracturing data. The formation water density is normally 0.97–1.07 g/cm^3.

The above mathematical model of the overpressure rupture coefficient (f) is based on 288 measured rupture pressure data from well logs (Fig. 2).

According to the data in Figure 2, the fracture pressure profiles of shale in the eastern and central-western China are clearly different. At the same depth, the fracture pressure in the central-western regions is significantly higher than in the eastern regions. The data points of

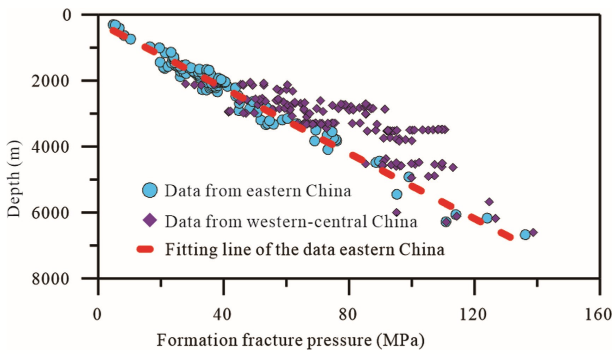

Fig. 2. Section diagram of the relationship between measured formation fracture pressure and burial depth in drilling.

fracture pressure in central-western China deviate above from the linear-fitting trend line of fracture pressure data in eastern China. The fracture pressure gradient of shale in central-western China is clearly greater than that in eastern China, which is generally greater than 2.0, reflecting the influence of the local tectonic stress, that increases the shale hydraulic fracture pressure. There must exist a value which can reflect the extent of deviation resulting from the tectonic stress field. After much trial and error, it was determined that the value is nearly equal to half of the additional tectonic stress coefficient (K_h). To verify if formulae (2) and (3) were reliable, the measured data were compared with the calculated data, showing that the average absolute error between the overpressure rupture coefficient determined by the above identification index determination method and the measured value of horizontal hydraulic fracturing in shale gas exploration wells was between 0.022 and 0.173, which demonstrates a high level of accuracy (see Fig. 3).

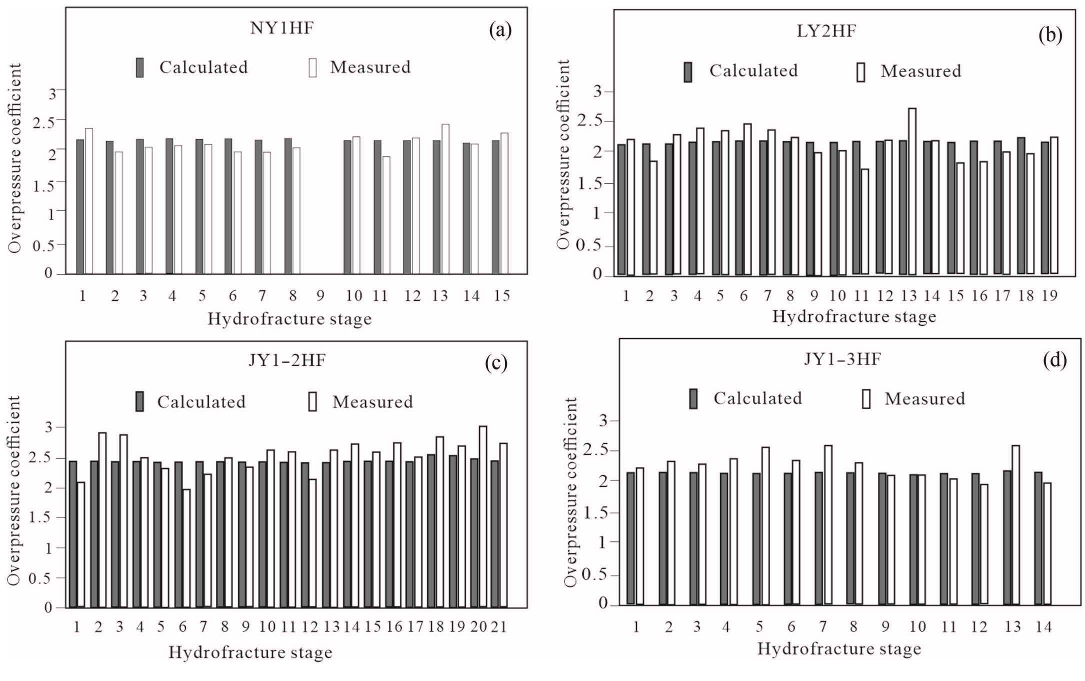

Fig. 3. Histogram comparison showing the errors between the measured and calculated overpressure coefficients in hydraulic fracturing shale gas exploration wells in the Sichuan Basin.

(3) Overconsolidation ratio (OCR)

According to the definition of OCR, the ratio between the maximum effective vertical stress and the present effective vertical stress (Nygard et al., 2006):

$$OCR = \frac{\sigma'_{v\max}}{\sigma'_v} \approx \frac{(\rho_1 - 1.07)H_{\max}}{(\rho_2 - 1.07)H_{present}} \tag{4}$$

where ρ_1 is the average density of overlying strata at the maximum burial depth in g/cm^3; ρ_2 is the average density of the current overlying strata, g/cm^3; $H_{\max}$, maximum ancient burial depth, m; H_{present}, present burial depth, m. Let the formation water density be 1.07 g/cm^3.

The larger the OCR is, the greater the brittleness. The closer the OCR is to 1, the larger the ductility, the higher the degree of fracture healing by the overlying vertical effective stress and the more the integrity of the caprock is repaired.

(4) Bottom boundary of the shale brittle zone (Z_b)

After the OCR threshold value was obtained by uniaxial strain and triaxial compression tests, the bottom boundary of the brittle zone can be calculated from the maximum vertical effective stress, which can be reconstructed from the burial history. The maximum paleo-burial depth can be obtained from the burial history reconstruction, the maximum vertical effective stress then being calculated from the maximum paleo-burial depth. As the OCR is defined as the ratio between the maximum effective vertical stress and the present-day effective vertical stress:

$$OCR = \sigma'_{v\max} / \sigma'_v \approx [(\rho_{r\max} - \rho_w)gH_{\max}] / [(\rho_{rpresent} - \rho_w)gH_{present}] \tag{5}$$

when the OCR reaches the threshold value, the present burial depth is simply the bottom boundary of the brittle zone (Z_b) (Yuan et al., 2017).

$$Z_b \approx \frac{Z_{\max}}{OCR_{threshold}} \tag{6}$$

With the increase of uplifting denudation, OCR increases. When the OCR increases to a certain value, the shale becomes completely brittle and brittle fracture is likely to occur, resulting in a large number of tensile fractures. That is to say, when the shale is uplifted to the bottom of the brittle zone, it will completely lose the ability to seal gas.

(5) Top boundary of the ductility zone (Z_d)

The depth converted from the critical confining pressure of brittleness is the top boundary depth of the ductility zone (Yuan et al., 2017). That is:

$$Z_d = 100 \times P_{b\text{–}d} / (\rho_r - \rho_w) \tag{7}$$

where H_d is the top boundary depth of the ductility zone, m; $P_{b\text{–}d}$ is the critical confining pressure of the brittle-ductile transition, MPa; ρ_r is the density of the overlying strata, g/cm^3. P_w is the water density, g/cm^3. The critical confining pressure above can be obtained through the uniaxial strain test (Addis, 1987).

(6) Fracture healing depth (Z_c)

The destruction of petroleum reservoir preservation conditions though folding, faulting or uplifting denudation is due to the integrity of the caprocks being compromised by fractures/faults. When the tectonism that caused the fractures disappears, the deeply buried shale fracture can be closed by the weight of the overlying strata, so that the integrity of the caprock can be repaired. The results of the shale permeability test under confining stress show that when the overlying vertical effective stress increases from 0 MPa to 15–25 Mpa, the permeability of shale samples decreases rapidly, while the confining pressure increases from 15–25 MPa to 60 MPa, the permeability of shale samples basically remaining unchanged (Yuan et al., 2020). It can be considered that the fracture of the Silurian Longmaxi Formation is closed under a vertical stress of about 15–25 MPa. This is named the critical confining pressure of the brittle-ductile transition ($P_{b\text{-}d}$). The $P_{b\text{-}d}$ value of 15–25 MPa translates into a depth of roughly 1000–1600 m. Then, if the stratum is inclined, the component of the vertical effective stress on the fracture plane should also reach 15–25 MPa (Yuan et al., 2020). At this point, the healing depth of the fractures is no less than the fracture healing depth (Z_c):

$$Z_c = 15/[(\rho_r - \rho_w)\,g\cos\alpha] \tag{8}$$

where Z_c is the healing depth of fractures through overlying vertical effective stress, m; ρ_r is the average density of overlying rock strata, g/cm^3; ρ_w is the formation water density in the overlying strata, g/cm^3; g is the acceleration of gravity, m/s^2; α is the fracture inclination angle. In other words, the greater the fracture inclination angle α, the greater the burial depth required for shale fracture healing.

(7) Fault sealing index (I)

There are many factors that affect fault sealing. For Meso-Cenozoic rocks with low diagenetic evolution, lithological alignment and mudstone smearing are the main factors, for which there are mature evaluation indexes associated with these factors (Allan, 1989; Fu et al., 2015). For the sealing evaluation of the ultra-deep fault, the combination of fault sealing index (I) and OCR can be considered suitable. The fault sealing index is the ratio of the normal stress on the fault surface to the formation fluid pressure (Wang and Dai, 2012). When I is greater than 1 and the OCR is small, which is at least less than the OCR threshold value of the shale, the fault is capable of sealing and containing oil and gas. The closer the OCR is to 1, the higher the fault healing degree is; otherwise, the fault does not have the ability to seal and contain gas, or simply performs poorly as a seal.

$$I = \frac{\delta_n}{f\rho_w g Z} \tag{9}$$

where I is the healing fault sealing index, dimensionless; σ_n is the normal stress perpendicular to the fault plane, MPa, f is the formation fluid pressure coefficient, dimensionless; ρ_w is the formation water density, g/cm^3; g is the acceleration of gravity, m/s^2; Z is the burial depth, m.

(8) Diffusion coefficient of caprock under formation conditions

The Lower Cambrian shale samples in the Sichuan Basin were collected to test diffusion coefficients under different confining pressures and temperatures. The gas diffusion coefficient data was measured by a self-designed and developed device that can automatically track and maintain the pressure of diffusion chambers at both ends at a constant, keeping the pressure difference close to zero (≤0.01 MPa). It can simulate formation temperatures and pressures at greater depths than previously possible. The maximum experimental temperature of the instrument is 180°C, the maximum experimental gas pressure (equivalent to pore pressure) is about 70 MPa, the maximum confining pressure being able to reach 100 MPa (Lu et al., 2020).

This shows that there is a good correlation between the diffusion coefficient of shale caprock and burial depth, which is converted from confining pressure (Fig. 4). According to the linear fitting result from the data shown in Figure 2, when the burial depth (Z) is known, the diffusion coefficient (D) can be roughly estimated, according to:

$$D = 1307 \times Z^{-0.94} \quad (10)$$

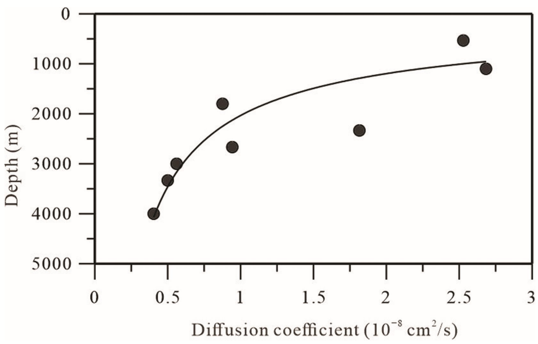

Fig. 4. Relationship between diffusion coefficient of lower Cambrian shale and current burial depth in the Sichuan Basin.

3.2 Chemical loss evaluation index and determination methods

3.2.1 Evaluation index and determination method for TSR hydrocarbon loss

ZnPVT is used to represent the gas reservoir state parameters, Z, N, P, V and T, which respectively represent the deviation coefficient of natural gas (dimensionless), the amount of natural gas per unit volume of the reservoir (mol), the gas reservoir pressure (MPa), the volume of natural gas per unit volume of the reservoir and the reservoir temperature (K). According to the burial depth and temperature of the reservoir, three states of the gas reservoir in geological history are established (Fig. 5).

State 1 is the state at the present burial depth ($Z_1n_1P_1V_1T_1$). State 2 is the state ($Z_2n_2P_2V_2T_2$) at the maximum paleo-burial depth of the reservoir when TSR is considered. State 3 is the state when the reservoir reaches the maximum paleotemperature or 210° C, without considering TSR ($Z_3n_3P_3V_3T_3$). State 3 is fictitious and did not exist, because TSR has been occurring since 120°C and hydrocarbon consumption and oil pyrolysis occur simultaneously within the oil cracking temperature window (160–210°C). State 2 contains the effect of TSR, its $n_2P_2V_2$ parameter mainly being determined by the dynamic coupling relationship between the pressurization of oil cracking to gas and the decompression of hydrocarbons being consumed by TSR. From state 2 to state 1, the changes in the gas reservoir temperature and pressure are mainly caused by uplift denudation. It is assumed that during late uplift denudation and reservoir temperature reduction, TSR's hydrocarbon loss stops, the caprock sealing ability is excellent and the reservoir is completely sealed during uplift. Therefore, from the maximum paleo-burial depth to the present, the change of gas reservoir pressure is only controlled by gas volume expansion/contraction caused by the pore rebound of uplift unloading and reservoir cooling. The temperature/pressure parameters of state 1 (P_1/T_1) are all known quantities. Therefore, starting from state 1, the pressure of state 2 (P_2) can be inversely obtained, according to the pore rebound of uplift unloading and the volume contraction of the reservoir cooling gas. The pressure parameter of state 3 (P_3) was determined by the paleo-pressure corresponding to the maximum homogenization temperature of the reservoir saline inclusions.

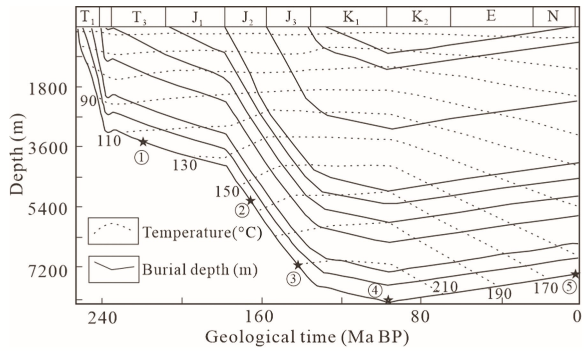

Fig. 5. Schematic diagram of three states in geological history setting for TSR.

1–TSR onset; 2–Oil cracking onset; 3–State 3, oil cracking end; 4–State 2, maximum burial depth; 5–State 1, present-day burial depth.

For a particular gas reservoir, according to the nonideal gas equation of state, in state 1 there exists:

$$P_1V_1 = Z_1n_1RT_1 \quad (11)$$

$$\text{i.e., } f_1\rho_w gH_1\phi_1VS = Z_1n_1RT_1 \quad (12)$$

$$\text{in state 2, } P_2V_2 = Z_2\,n_2RT_2 \quad (13)$$

$$\text{i.e., } f_2\rho_w gH_2\phi_2VS = Z_2n_2RT_2 \quad (14)$$

$$\text{in the state 3, } P_3V_3 = Z_3\,n_3RT_3 \quad (15)$$

$$\text{i.e., } f_3\rho_w gH_3\phi_3VS = Z_3n_3RT_3 \quad (16)$$

then, TSR hydrocarbon degree of loss can be expressed by the parameter N:

$$N = 100 \times (1 - n_2/n_3) = 100 \times (1 - (f_2 \bullet H_2 \bullet \phi_2 \bullet T_3 \bullet Z_3)/(f_3 \bullet H_3 \bullet \phi_3 \bullet T_2 \bullet Z_2)) \quad (17)$$

Among them, P_1 (Pa), V_1 (m^3), T_1 (K), n_1 (mol), H_1 (m), Z_1 (dimensionless), R (dimensionless), f_1 (dimensionless), ϕ_1 (decimal), V (m^3) and S (decimal), are gas reservoir pressure, gas volume per unit volume of reservoir, reservoir temperature, gas amount per unit volume of reservoir, burial depth of reservoir, deviation coefficient of natural gas, universal gas constant, gas reservoir pressure coefficient, gas volume per unit volume of reservoir, and gas saturation under current geological conditions. P_2 (Pa), V_2 (m^3), T_2 (K), n_2 (mol), H_2, (m), Z_2, f_2 (dimensionless), P_3 (Pa), V_3 (m^3), T_3 (K), n_3 (mol), H_3 (m), Z_3 (dimensionless) and f_3 (dimensionless) are the corresponding parameters of state 2 and state 3, respectively.

3.2.2 Evaluation index and determination method for TOH hydrocarbon loss

There are two main indexes to identify the oxidized hydrocarbons of high-valence iron and manganese oxides. One is isotopic index, including authigenic calcite $\delta^{13}C$ and $\delta^{18}O$. The other is manganese content, mainly MnO content in authigenic calcite. In other words, in the deep/ultra-deep geological environment, when the authigenic calcite $\delta^{13}C$ formed by methane oxidation and CO_2 precipitation in the 'bleached' reservoir is extremely negative, $\delta^{18}O$ is also negative and the MnO content is significantly increased, it can be determined that the hydrocarbons have been oxidized by high-valence manganese oxides. Taking the Lower Triassic Baikouquan Formation in Mahu Sag, Junggar Basin, as an example, the determination methods of these two kinds of indicators can be described.

The stable carbon isotope values of authigenic calcite formed by CO_2 precipitation from hydrocarbons oxidized by high-valence Fe and Mn oxides are extremely negative. The $\delta^{13}C$ values of whole rock calcite in the Baikouquan Formation range from −22.47‰ to −69.76‰, with the main calcite range extending from −36.0‰ to −50.0‰. The $\delta^{13}C$ of authigenic calcite is 19‰–24‰ lower than that of methane. The $\delta^{18}O$ of authigenic calcite also has a negative bias trend, its distribution ranging from −12.81‰ to −22.60‰ (Hu et al., 2018), which is similar to that of $\delta^{13}C$. In-situ carbon isotope analysis of calcite shows that the $\delta^{13}C$ difference between the two phases is up to 10‰, the average value being basically the whole rock test value, while the in-situ $\delta^{18}O$ difference is slightly smaller, the maximum difference being only 1.86‰.

In terms of chemical composition, the authigenic calcite associated with hydrocarbons oxidized by high-valence Fe and Mn oxides is generally Mn-rich. MnO content in the Baikouquan Formation ranges from 0.79% to 14.67%, with an average of 5.05%. The MnO content of early calcite is generally lower than 4.00% and mostly less than 2.00%, while the MnO content of late coarse-grained calcite is generally greater than 5.00% and the high value can reach 11.00%–15.00% (Hu et al., 2018). In contrast, the FeO content is relatively low, which is 0.01%–0.79%, with an average of 0.12%. FeO content of calcite in different periods is also different, but the trend is not as obvious as that of Mn.

The above examples can be used as a reference for evaluating the chemical loss of hydrocarbons, but the quantitative relationship between the degree of loss of TOH hydrocarbons and the negative $\delta^{13}C$ or MnO content of authigenic calcite in specific areas requires further research.

4 Evaluation Index System of Ultra-deep Hydrocarbon Preservation, with Case Studies

4.1 Evaluation index system of ultra-deep hydrocarbon preservation

In summary, the evaluation index system of ultra-deep preservation conditions involves physical leakage and chemical loss. Including the microscopic dynamic effectiveness of caprocks, caprock integrity related to fault sealing and fracture associated with shale caprocks, gas diffusion under high temperature and high pressure, TSR hydrocarbon loss in marine carbonate reservoirs and TOH hydrocarbon loss in clastic strata. In total, the evaluation index system of ultra-deep oil and gas preservation conditions involves 12 indexes:

1) *SCM*, source/caprock matching relationship, which is a term for evaluating the microscopic dynamic validity of caprocks; *SCM* occurs as one of 3 types, i.e., source/caprock completely matching; source/caprock partially matching; source/caprock not matching;

2) *I*, fault stress sealing index, which is a term for evaluating fault sealing capability; $I = \sigma_n/f\rho_w gZ$; when the value of *I* is greater than 1 and *OCR* is much smaller than the $OCR_{\text{threshold}}$, the fault is capable of sealing hydrocarbons;

3) θ, bedding slip angle; $\theta = 45-\phi/2$, when the formation dip angle is consistent with the bedding slip angle, bedding slip crack is likely to occur and caprock integrity will be compromised;

4) Z_b, bottom boundary of the brittle zone; when the burial depth of the caprock is above Z_b, it is likely to produce brittle cracks and caprock integrity will be compromised;

5) Z_d, top boundary of the ductile zone; when the burial depth of the caprock is below the ductile zone, it is not likely to produce brittle cracks and has good integrity;

6) Z_c, healing depth of fracture by overlying strata; when the burial depth of the caprock is below the healing depth, the fracture of the caprock will to some extent be closed;

7) *OCR*, overconsolidation ratio; the degree of fracture healing is related to OCR. The smaller the OCR, the higher the degree of fracture healing;

8) *f*, overpressure rupture coefficient; when the formation fluid pressure coefficient is greater than the overpressure rupture coefficient of the caprock, the caprock is broken and its integrity is destroyed;

9) *D*, diffusion coefficient; $D = 1307 \times Z^{-0.94}$. It can be roughly estimated according to the burial depth of the caprock;

10) *N*, chemical loss evaluation of TSR; hydrocarbon loss by TSR can be quantitatively evaluated according to *N*;

11) $\delta^{13}C/\delta^{13}C_1$, chemical loss evaluation of TOH; the difference or ratio between $\delta^{13}C$ of authigenic calcite and $\delta^{13}C_1$ of methane, is based on the degree of $\delta^{13}C$ deviation of authigenic calcite to evaluate the degree of hydrocarbon depletion of TOH;

12) *ACCC*, authigenic calcite cement content, which also relates to chemical loss evaluation of TOH.

4.2 Case studies

The index assessment system for ultra-deep oil and gas preservation conditions evaluation is quite extensive and the determination methods are also rather complex. Therefore, for a particular exploration well or exploration zones, a simplified method of preservation condition evaluation is firstly provided through the analysis of geological conditions, focused on evaluating one or a few key indicators, without the need for all 12 indicators to be involved. Specifically, it can be roughly divided into the following four scenarios.

4.2.1 Gypsum is the caprock in an ultra-deep exploration area

In the ultra-deep exploration area, where gypsum is the caprock, the chemical loss evaluation of TSR hydrocarbon should be emphasized, while the physical leakage needs only a qualitative evaluation. Taking well YB-2, which is located in Cangxi county, Sichuan province, as a case study, this Is part of the Bazhong low and slow structural belt in the northeast of the Sichuan Basin. The topmost layer is purple red mudstone of the Cretaceous, the drilling depth being 6828 m. The present burial depth of the Changxing Formation is 6720 m, its maximum paleo-burial depth being 7519 m according to the burial history reconstruction. The gypsum of well YB-2 is well-developed. The drilling and logging data shows that the accumulated thickness of gypsum from the top of the Jialingjiang Formation to the fourth member of the Feixianguan Formation in the Lower Triassic (T_1f^4) is 250.5 m. The thickness of the single layer is larger than 3.0 m in general, the maximum thickness of a single layer can reach 52.0 m according to the drilling data, which can form a good seal for the lower sequences. The Changxing Formation natural gas in well YB-2 is an acidic gas with H_2S content of 3.8%–4.4%, H_2S + CO_2 content 12.6%–15.3%. The methane content is 83.2%–85.6% and the ethane content is 0.06%–0.13% (Li et al., 2016), so it is necessary to carry out hydrocarbon chemical loss evaluation. Using the ZnPVT state parameter method to calculate the TSR hydrocarbon loss degree $N = 100 \times (1 - n_2/n_3) = 20\%$ in well YB-2 gas field, that is, the hydrocarbon loss caused by TSR in well YB-2 gas field is about 20% of the initial gas reservoir reserves (Table 2).

4.2.2 Shale is the caprock in an ultra-deep exploration area

In ultra-deep exploration areas where shale acts as the caprock, it has a good micro-sealing capability, small OCR, high degree of overlying fracture healing and good integrity. However, the caprock is not necessarily dynamic effective. Therefore, it is sometimes necessary to evaluate the dynamic effectiveness of micro-sealing, such as well GS-1 in the southwest of the Sichuan Basin.

Well GS-1 is located on the Tiangongtang anticline, about 23 km east of Wuzhishan, southwest Sichuan Basin. The drilling maximum depth is 4980 m, reaching the strata of the third member of the Sinian Dengying Formation (Z_2^3) and no industrial oil or gas flow was obtained. The source rocks of the Lower Cambrian Qiongzhusi Formation and the Lower Silurian Longmaxi Formation were developed in the lower Paleozoic in well GS-1. From Figure 6, data obtained from the capillary pressure reconstruction method (Jin et al., 2014), it can be seen that the capillary pressure at the bottom of the Lower Cambrian shale caprock was 2.6 MPa at the end of the early Paleozoic, which had good oil sealing capability. At the end of the late Permian, it was larger than 5 MPa and had the ability to act as a seal for natural gas. By the end of the Middle Triassic, the capillary pressure was more than 10 MPa and the high-pressure gas reservoir could be sealed. The capillary pressure reached 15 MPa at the end of the Early Cretaceous, sealing the ultra-high pressure gas reservoir and reaching its maximum value (18.5 MPa) at the end of the Oligocene. Since the Oligocene, the caprock capillary pressure has decreased due to uplift and denudation, the capillary pressure dropping back to 12.0 MPa at the end of the Neogene. From the perspective of the micro-parameter of capillary pressure, it can be concluded that the Cambrian shale caprock in well GS-1 still has the ability to seal high-pressure gas reservoirs. Another set of argillaceous caprocks in well GS-1 is the Lower Silurian Longmaxi Formation shale. The capillary pressure of the argillaceous caprock of the Longmaxi Formation is 2.6 MPa at the end of the early Paleozoic, which is capable of sealing oil. At the end of the Middle Jurassic, the capillary pressure reached 5 MPa and it began to have the ability of sealing natural gas. At the end of the Late Cretaceous, the capillary pressure reached 10 MPa, which could seal the high-pressure gas reservoir. At the end of the Oligocene, the capillary pressure reached its maximum value (12.3 MPa). Since the Oligocene, due to uplift and pressure relief, the caprock capillary pressure decreased, dropping to 4.8 MPa at the end of the Neogene. From the perspective of the micro-parameter of breakthrough pressure, the sealing ability of the Silurian Longmaxi Formation caprock in well GS-1 was greatly weakened in the uplift stage and its sealing ability is poor at present (Fig. 6).

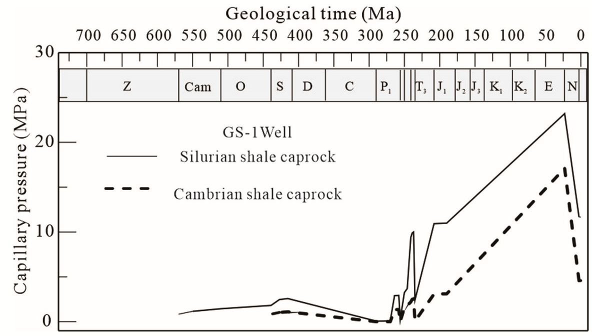

Fig. 6. Capillary pressure (*P*c) history of the shale caprock in Well GS-1 in the southwest of the Sichuan Basin.

The average content of residual organic carbon in the Cambrian Qiongzhusi and the Lower Silurian Longmaxi formations is about 0.78% and 1.31% respectively in well GS-1. The calculation results of the hydrocarbon generation history of well GS-1 show that the oil generation period of the Cambrian Qiongzhusi Formation is from the Middle Cambrian to the late Silurian, the main gas generation period from kerogen being from the Devonian to the Early Permian and the dispersed hydrocarbon cracking to gas is from the Carboniferous to the Early Permian. Under conditions of high heat flow and high temperatures during the Early Permian, the source rocks of the Lower Cambrian Qiongzhusi Formation rapidly matured and generated hydrocarbons. The degree of thermal evolution of organic matter (*R*o) rapidly increased from 0.7% to more than 3.5% during the Early Permian. The source rock no longer had hydrocarbon generating potential by the end of the Permian.

The dynamic matching relationship between source and caprock in well GS-1 is not ideal for reservoir formation.

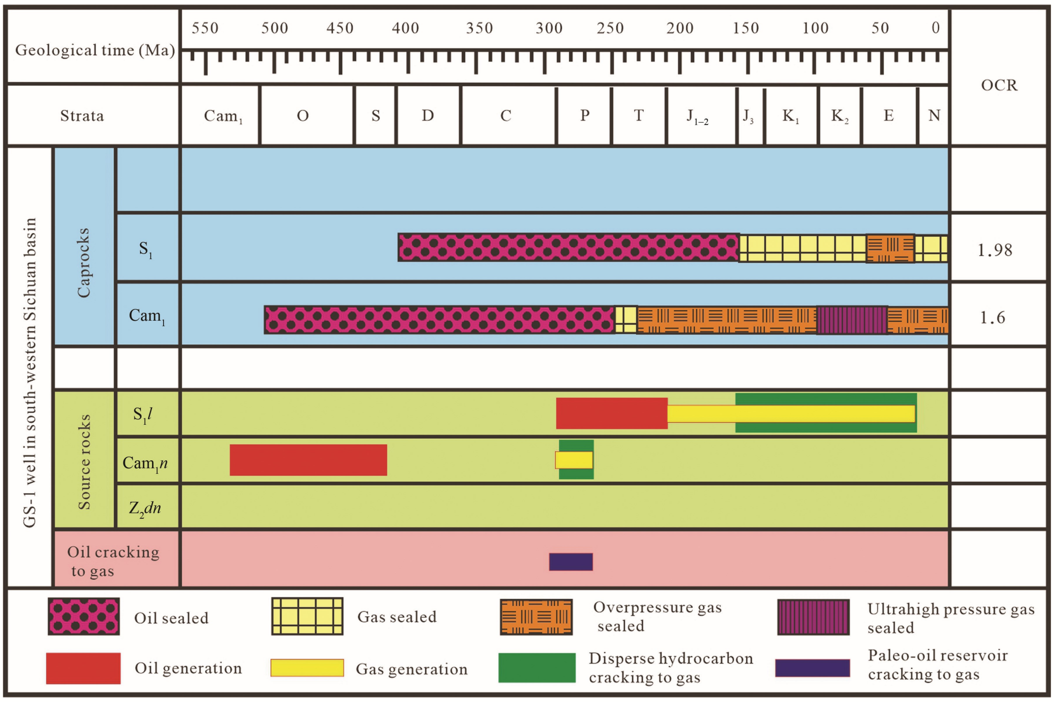

Fig. 7. Diagram showing dynamic matching of source/caprock of Well GS-1 in southwest China.

Due to the Lower Cambrian source rock being close to the middle belt of the Emeishan basalt eruption area (Xu et al., 2020), under high heat flow and temperature, it rapidly matured and generated hydrocarbons. The kerogen matured sharply and the vitrinite reflectance reached more than 3.5% by the end of the Early Permian, the hydrocarbon generating potential being exhausted. The paleo-oil reservoirs in the Sinian system, which were derived from Cambrian hydrocarbon source rock, also cracked and generated gas rapidly in this period, resulting in a short hydrocarbon generation period, when the sealing capacity had not yet formed, so was unfavorable to hydrocarbon accumulation (Fig. 7). There was no oil and gas found in well Gongshen-1. The unsatisfactory source/caprock matching relationship may be one of the important reasons for this. Both the hydrocarbon generation time of the source rock and the oil cracking time of the paleo-oil reservoir are earlier than the sealing formation time of the caprocks.

4.2.3 Shale is the caprock of an exploration area with significant uplift and denudation in a later period

In regions with extensive uplift and denudation in a later period, the caprock had experienced ultra-deep paleo-burial depths within geological history, but the present burial depth is not necessarily ultra-deep. It is important to evaluate the integrity of shale caprocks in such exploration zones. Well PY-1 in the Pengshui area, southern China, can be used as an example to show the methods of estimating preservation.

The topmost stratum of well PY-1 is the Daye Formation of the Lower Triassic system. The base drilling stratum is the Baota Formation, with a depth of 2208 m. The bottom depth of the Silurian Longmaxi Formation is 2153 m. The average density of the overlying rocks is 2.65 g/cm^3, the overlying pressure from the strata being around 55 MPa, with a vertical effective pressure of about 32 MPa. The maximum paleo-burial depth of the bottom of the Longmaxi Formation is about 5971 m, according to burial history reconstruction, the vertical effective pressure at the maximum burial depth being about 89 MPa, which is reduced by 57 MPa due to uplift and denudation. The denudation amount is about 3700 m, the hydrostatic pressure decreasing by 37 MPa after uplift. In the Early Cretaceous, the paleotemperature reached 206°C, according to temperature history reconstruction, the present temperature at the bottom of the well being 66°C. After uplift, the temperature decreased by 140°C (Fig. 8).

During the uplift process, the absolute value of the fluid pressure decreased, but the vertical stress decreased, due to the denudation of the overlying strata, so the fluid pressure coefficient increased. Prior to the uplift, the pressure coefficient of the Longmaxi Formation was 1.4–1.6, according to the fluid inclusions. During the uplift, the pressure coefficient of the Longmaxi Formation exceeded 2.0 (Fig. 9), based on the fluid pressure molding, resulting in overpressure rupture and natural gas loss. In addition, the dip angle of the Longmaxi Formation is 10°–30°, which is likely to produce bedding shear fractures. The OCR of the Longmaxi shale is 2.9, which is characterized by brittle fracture, the fractures being difficult to close completely under the overlying strata.

It can be seen that the late uplift and denudation of Well PY-1 was intense, overpressure fracture occurring in the caprock during the uplift process. In addition, the dip angle of the Longmaxi Formation meeting its bedding slippage angle, which is prone to produce bedding slip fractures and damage to the integrity of the caprock. At the same time, the Longmaxi shale is of large OCR value above the brittle fracture threshold (2.6), resulting in a low

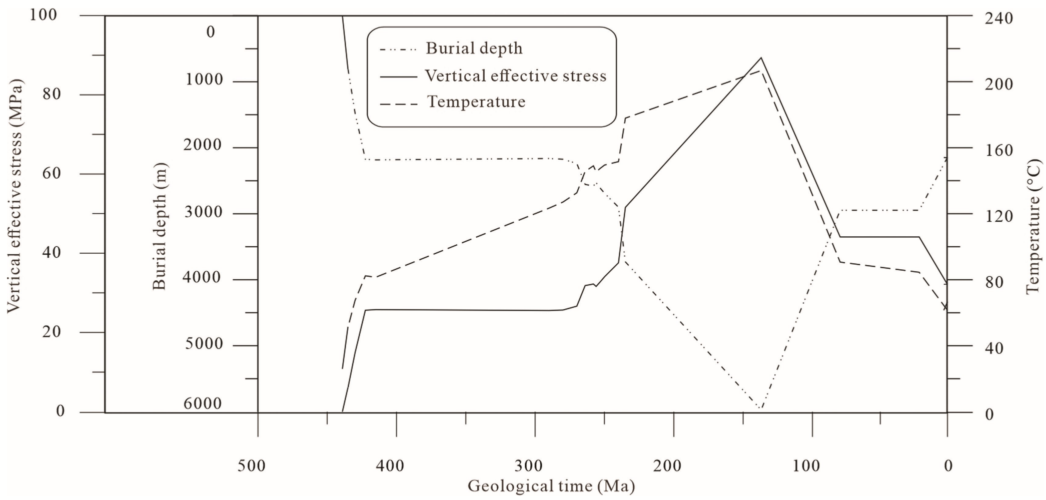

Fig. 8. Graph showing evolution of temperature and vertical effective stress of the Longmaxi Formation in well PY-1.

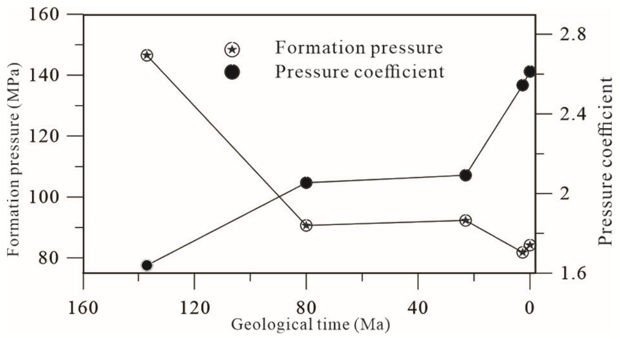

Fig. 9. Graph showing the evolution of the Silurian Longmaxi Formation pressure and pressure coefficient in well PY-1.

degree of fracture healing and damage of caprock integrity, therefore the preservation conditions were seriously damaged, so that the degree of loss of the shale gas of the Longmaxi Formation in PY-1 well being bigger, the formation pressure of the Longmaxi shale changing from high pressure to normal pressure, resulting in low shale gas production.

4.2.4 Ultra-deep clastic rock exploration areas

For ultra-deep clastic rock exploration areas, shale is usually the main caprock. In addition to the evaluation of the dynamic effectiveness of microscopic sealing of caprocks, the chemical loss of high-valence metallic minerals to hydrocarbons is also worth paying attention to. This is particularly the case in the reservoirs with 'bleaching' phenomena, such as the obvious 'bleaching' phenomenon in part of the Baikouquan Formation in the Mahu Sag of the Junggar Basin, where hydrocarbon TOH loss in this area should have specific attention paid to it. However, the quantitative evaluation method of hydrocarbon TOH loss has not at present been established and the current work can only provide an evaluation concept. The quality of authigenic calcite is first determined by counting the strata and content of authigenic calcite in the reservoir, then the CH_4 loss is calculated, according to the amount of CH_4 required to produce authigenic calcite per unit mass. The other method is to evaluate the chemical loss of hydrocarbons qualitatively or semi-quantitatively, by establishing the relationship between the decrease of $\delta^{13}C$ in authigenic calcite and the loss of CH_4.

5 Conclusions

On account of the high temperatures, high pressures and high in-situ stresses in the ultra-deep environment of sedimentary basins, it is necessary to evaluate the oil and gas preservation conditions, both in terms of physical leakage and chemical loss.

The physical leakage evaluation indexes can be divided into three categories: first, the dynamic efficiency indexes of caprock micro-sealing; second, the integrity index of caprock evaluation; third is the gas diffusion index. The slippage angle and overconsolidation ratio (OCR) are the key evaluation indexes in the evaluation of the integrity of shale caprocks. The former determines the possibility of slippage fracture occurring along the bedding plane, while the latter determines the healing degree of the fractures by overlying strata. The smaller the OCR, the higher the healing degree of cracks in shale caprocks and, therefore, the more the integrity of the caprocks is repaired. In contrast, when the OCR is greater than the brittle fracture threshold value, the integrity of the caprocks is very likely to be compromised.

The chemical loss evaluation indexes for ultra-deep oil and gas conservation can be divided into two categories: the TSR index in marine gypsum-bearing carbonate strata and the TOH index in clastic strata. TSR related hydrocarbon loss can be quantitatively evaluated by the ZnPVT state parameter method, while TOH related chemical loss can be evaluated by the relationship between the amount of authigenic calcite or the degree of $\delta^{13}C$ reduction and CH_4 loss, but further study is needed in this regard.

The TSR hydrocarbon loss evaluation is the focus of the ultra-deep exploration area with gypsum as the caprock. In ultra-deep exploration areas with shale caprock, the evaluation of microscopic sealing dynamic effectiveness is sometimes key. It is particularly important to evaluate the integrity of shale caprock in the areas with extensive uplift and denudation in the later period. For ultra-deep clastic rock exploration areas, attention should be paid not only to the microscopic sealing dynamic effectiveness of the caprocks, but also to the chemical loss evaluation of oxidized hydrocarbons of high-valence metallic minerals.

Nomenclature

TSR–Thermochemical Sulfate Reduction;
TOH–Thermochemical Oxidation of Hydrocarbon;
SCM–Source/caprock matching relationship;
ACCC–Authigenic calcite cement content (%);
OCR–Overconsolidation ratio, dimensionless;
I–Fault sealing index; dimensionless;
θ–Bedding slippage angle of shale caprock (°);
α–Fracture inclination angle (°);
Φ–Internal friction angle (°);
f–Overpressure rupture coefficient, dimensionless;
Z_b–Bottom boundary of brittle zone (m);
Z_d–Top boundary of ductility zone (m);
Z_c–Fracture healing depth (m);
D–Diffusion coefficient (cm^2/s);
K_h–Additional tectonic stress coefficient along the direction of minimum horizontal principal stress; dimensionless;
ρ_w–Formation water density (g/cm^3);
ρ_r–Density of overlying strata (g/cm^3);
ρ_{max}–Density of the overlying rocks when the caprock was buried at its maxmum depth (g/cm^3);
Z_{max}–Maximum ancient burial depth (m);
$Z_{present}$–Present burial depth (m);
G–Acceleration of gravity (m/s^2);
σ'_{vmax}–Maximum effective vertical stress (MPa);
σ'_v–Present-day effective vertical stress (MPa);
$OCR_{threshold}$–*OCR* threshold value; Dimensionless;
$P_{b\text{-}d}$–Critical confining pressure of brittle-ductile transition (MPa);
σ_n–Normal stress perpendicular to the fault plane (MPa);
Z–Deviation coefficient of natural gas in the ultra-deep environment, dimensionless;
n–Amount of natural gas per unit volume of the reservoir (mol);
P–Gas reservoir pressure (MPa);
V–Volume of natural gas per unit volume of the reservoir, dimensionless;
T–Reservoir temperature (K);
N–Hydrocarbon chemical loss related to TSR (%).

Acknowledgments

This research was financially supported by the National Key R & D Program of China (Grant No. 2017YFC0603105). Many thanks to the reviewers for their numerous useful comments, that helped improve the manuscript.

Manuscript received Jan. 11, 2022
accepted Jun. 11, 2022
associate EIC: ZHANG Shuichang
edited by Jeffery J. LISTON and FANG Xiang

References

Addis, M.A., 1987. Mechanisms for sediment compaction responsible for oil field subsidence (Ph.D. thesis). UK: University of London.
Allan, U.S., 1989. Model for hydrocarbon migration and entrapment within faulted structures. AAPG Bulletin, 73(7): 803–811.
Amann, F., Kaiser, P., and Button, E.A., 2012. Experimental study of brittle behavior of clay shale in rapid triaxial compression. Rock Mechanics and Rock Engineering, 45(1): 21–33.
Bolton, A.J., Maltman, A.J., and Clennell, M.B., 1998. The importance of overpressure timing and permeability evolution in fine-grained sediments undergoing shear. Journal of Structural Geology, 20(8): 1013–1022.
Cai, C., and Li, H., 2005. Thermochemical sulfate reduction in sedimentary basins: A review. Advances in Earth Science, 20 (10): 1100–1105 (in Chinese with English abstract).
Cai, C., Xiang, L., Yuan, Y., Xu, C., He, W., Tang, Y., and Borjigin, T., 2017. Sulfur and carbon isotopic compositions of the Permian to Triassic TSR and non-TSR altered solid bitumen and its parent source rock in NE Sichuan Basin. Organic Geochemistry, 105: 1–12.
Cai, C., Zhang, C., He, H., and Tang, Y., 2013. Carbon isotope fractionation during methane-dominated TSR in East Sichuan Basin gasfields, China: A review. Marine and Petroleum Geology, 48: 100–110.
Chen, M., Kang, Y., Zhang, T., You, L., Li, X., Chen, Z., Wu, K., and Yang, B., 2018. Methane diffusion in shales with multiple pore sizes at supercritical conditions. Chemical Engineering Journal, 334: 1455–1465.
Chitrala, Y., Moreno, C., Sondergeld, C., and Rai, C., 2013. An experimental investigation into hydraulic fracture propagation under different applied stresses in tight sands using acoustic emissions. Journal of Petroleum Science and Engineering, 108: 151–161.
Cobbold, P.R., Zanella, A., Rodrigues, N., and Løseth, H., 2013. Bedding-parallel fibrous veins (beef and cone-in-cone): Worldwide occurrence and possible significance in terms of fluid overpressure, hydrocarbon generation and mineralization. Marine and Petroleum Geology, 43: 1–20.
Dai, J.X., 2003. Pool-forming periods and gas sources of the Weiyuan gasfield. Petroleum Geology & Experiment, 25(5): 473–480 (in Chinese with English abstract).
Dehandschutter, B., Vandycke, S., Sintubin, M., Vandenberghe, N., Gaviglio, P., Sizun, J.P., and Wouters, L., 2004. Microfabric of fractured Boom Clay at depth: A case study of brittle-ductile transitional clay behaviour. Applied Clay Science, 26(1–4): 389–401.
Færseth, R.B., Johnsen, E., and Sperrevik, S., 2007. Methodology for risking fault seal capacity: Implications of fault zone architecture. AAPG Bulletin, 91(9): 1231–1246.
Faulkner, D.R., Jackson, C.A.L., Lunn, R.J., Schlische, R.W., Shipton, Z.K., Wibberley, C.A.J., and Withjack, M.O., 2010. A review of recent developments concerning the structure, mechanics and fluid flow properties of fault zones. Journal of Structural Geology, 32(11): 1557–1575.
Fu, G., and Su, Y., 2004. Geological factors controlling gas diffusion loss in strata section. Natural Gas Geoscience, 15(1): 58–61(in Chinese with English abstract).
Fu, X., Jia, R., Wang, H., Wu, T., Meng, L., and Sun, Y., 2015. Quantitative evaluation of fault-caprock sealing capacity: A case from Dabei-Kelasu structural belt in Kuqa Depression, Tarim Basin, NW China. Petroleum Exploration and Development, 42(3): 300–309 (in Chinese with English abstract).
Gueydan, F., Leroy, Y.M., and Jolivet, L., 2001. Grain-size-sensitive flow and shear-stress enhancement at the brittle–ductile transition of the continental crust. International Journal of Earth Sciences, 90(1): 181–196.
He, Z.L., Li, S.J., Wo, Y.J., Zhang, D.W., Gu, Y., and Zhou, Y., 2017. Major factors controlling hydrocarbon preservation condition in the marine basins of China and its evaluation ideas. Acta Petrologica Sinica, 33(4): 1221–1232 (in Chinese with English abstract).
Hu, W., Kang, X., Cao, J., Wang, X.L., Fu, B., and Wu, H., 2018. Thermochemical oxidation of methane induced by high-

valence metal oxides in a sedimentary basin. Nature Communications, 9(1): 31–51.
Jin, Z.J., Yuan, Y.S., Sun, D.S., Liu, Q.Y., and Li, S.J., 2014. Models for dynamic evaluation of mudstone/shale cap rocks and their applications in the Lower Paleozoic sequences, Sichuan Basin, SW China. Marine and Petroleum Geology, 49: 121–128.
Jin, Z.J., 2012. Formation and accumulation of oil and gas in marine carbonate sequences in Chinese sedimentary basins. Science China, Earth Sciences, 55(3): 368–385.
Jing, S., Dehua, L., Xiang, Z., Wenjun, H., and Liang, C., 2021. Experimental investigation on shale gas transport characteristics in nanopores under high temperature and high pressure. International Journal of Oil Gas and Coal Technology, 26(3): 302–325.
Kim, C., Jang, H., Lee, Y., and Lee, J., 2016. Diffusion characteristics of nanoscale gas flow in shale matrix from Haenam basin, Korea. Environmental Earth Sciences, 75(4): 1–8.
Krooss, B.M., Leythaeuser, D., and Schaefer, R.G., 1985. Experimental determination of diffusion parameters for light hydrocarbons in water-saturated rocks: Some selected results. Advances in Organic Geochemistry, 10: 291–297.
Krooss, B.M., Leythaeuser, D., and Schaefer, R.G., 1988. Light hydrocarbon diffusion in a caprock. Chemical Geology, 71(1–3): 65–76.
Larsen, B., and Gudmundsson, A., 2010. Linking of fractures in layered rocks: Implications for permeability. Tectonophysics, 492(1–4): 108–120.
Li, M.C., Li, W.C., and Feng, S.D., 1997. Integrative study of preservation conditions of oil and gas pools. Acta Petrolei Sinica, 18(2): 41–48 (in Chinese with English abstract).
Li, P., Hao, F., Guo, X., Zou, H., Zhu, Y., Yu, X., and Wang, G., 2016. Origin and distribution of hydrogen sulfide in the Yuanba gas field, Sichuan Basin, Southwest China. Marine and Petroleum Geology, 75: 220–239.
Lu, L., Wang, G., Zhu, H., Wang, G., and Jiang, T., 2020. The development of an experimental measuring apparatus for simulating the diffusion coefficient of natural gas in depth. Geophysical and Geochemical Exploration, 44(6): 1441–1445 (in Chinese with English abstract).
Lu, T.H. 2010. Soil Mechanics. Beijing: Higher Education Press.
Lv, Y., Chen, Z., Fu, G., Jiang, Z., and Chang, G., 1993. Research on displacement pressure of caprock. Journal of Daqing Petroleum Institute, 17(4): 1–8 (in Chinese with English abstract).
Ma, Y., Lou, Z., Guo, T., Fu, X., and Jin, A., 2006. An exploration on a technological system of petroleum preservation evaluation for marine strata in South China. Acta Geologica Sinica, 80(3): 406–417 (in Chinese with English abstract).
Ma, Y.S., and Zhao, P., 2016. Research progress in the petroleum and natural gas geological theory of China. Acta Geologica Sinica (English Edition), 90(4): 1236–1248.
Nankali, H.R., 2012. Brittle-ductile transition zone case study (Zagros–Iran). Journal of Asian Earth Sciences, 59: 156–166.
Nygard, R., Gutierrez, M., Bratli, R.K., and Kaare, H., 2006. Brittle-ductile transition, shear failure and leakage in shales and mudrocks. Marine and Petroleum Geology, 23(2): 201–212.
Rybacki, E., Meier, T., and Dresen, G., 2016. What controls the mechanical properties of shale rocks? – Part II: Brittleness. Journal of Petroleum Science and Engineering, 144: 39–58.
Song, J., and Zhang, D., 2013. Comprehensive review of caprock -sealing mechanisms for geologic carbon sequestration. Environment Science Technology, 47(1): 9–22.
Taghavinejad, A., Sharifi, M., Heidaryan, E., Liu, K., and Ostadhassan, M., 2020. Flow modeling in shale gas reservoirs: A comprehensive review. Journal of Natural Gas Science and Engineering, 83: 1–31.
Tarantola, A., Mullis, J., Vennemann, T., Dubessy, J., and Capitani, C.D., 2007. Oxidation of methane at the CH_4/H_2O-(CO_2) transition zone in the external part of the Central Alps, Switzerland: Evidence from stable isotope investigations. Chemical Geology, 237(3–4): 329–357.
Tarasov, B., and Potvin, Y., 2013. Universal criteria for rock brittleness estimation under triaxial compression. International Journal of Rock Mechanics and Mining Sciences, 59: 57–69.
Wan, Y., Bourdet, J., Hu, W., Kang, X., and Wang, X., 2021. Experimental investigations on the thermochemical oxidation of *n*-alkane and alcohol compounds by MnO_2 and Fe_2O_3 at temperatures up to 325°C. Chemical Geology, 559: 119982.
Wang, K., and Dai, J., 2012. A quantitative relationship between the crustal stress and fault sealing ability. Acta Petrolei Sinica, 33(1): 74–81.
Wang, K., Zhang, H., Zhang, R., Wang, J., Dai, J., and Yang, X., 2016. Characteristics and influencing factors of ultra-deep tight sandstone reservoir structural fracture: A case study of Keshen-2 gasfield Tarim Basin. Acta Petrolei Sinica, 37(6): 715–727 (in Chinese with English abstract).
Weber, J.K., Mandl, J.G., Pilaar, W. F., Lehner, B.V.F., and Precious, G.R., 1978. The role of faults in hydrocarbon migration and trapping in Nigerian growth fault structures. Houston: Off-shore Tech Conference Houston, Texas.
Xu, H., Gao, J.B., Yang, R.D., Du, L.J., Liu, Z.C., Chen, J., Feng, K.N., and Yang, G.H., 2020. Genesis for rare earth elements enrichment in the Permian manganese deposits in Zunyi, Guizhou Province, SW China. Acta Geologica Sinica (English Edition), 94 (1): 90–102.
Yuan, Y., Fan, M., Liu, W., Li, S., and Wo, Y., 2011. Several discussions of sealing capacity studies of caprock. Petroleum Geology & Experiment, 33(4): 336–340.
Yuan, Y., Jin, Z., Zhou, Y., Liu, J., Li, S., and Liu, Q., 2017. Burial depth interval of the shale brittle–ductile transition zone and its implications in shale gas exploration and production. Petroleum Science, 14: 637–647.
Yuan, Y., Sun, D., Zhou, Y., Wang, X., Li, S., Zhang, R., Wo, Y., and Zheng, H., 2010. Relationship between hydrocarbon generation history of source rocks and sealing history of mudstone cap-rocks in the southeast Sichuan Basin. Geological Review, 56(6): 831–838 (in Chinese with English abstract).
Yuan, Y., Fang, Z., He, X., Li, S., Peng, Y., and Long, S., 2020. Normal pressure formation mechanism of Longmaxi shale gas in Pengshui and its adjacent areas. Reservoir Evaluation and Development, 10(1): 9–16 (in Chinese with English abstract).
Yuan, Y., Hao, Y., Liu, Q., Gao, J., and Zhang, S., 2021. TSR hydrocarbon loss assessment: I. main controlling factors and intensity indicators of TSR. Marine oil and gas geology, 26 (2): 97–104 (in Chinese with English abstract).
Yuan, Y., Hu, W., Chen, S., and Wang, G., 2019. The main controlling factors and evaluation ideas of ultra-deep oil and gas preservation. Marine oil and gas geology, 24(4): 47–56 (in Chinese with English abstract).
Yuan, Y., Zhou, Y., Qiu, D., and Wang, Q., 2015. Evolutionary patterns of non-tectonic fractures in shale during burial. Oil & Gas Geology, 36(5): 822–827 (in Chinese with English abstract).
Zhang, S., and Tullis, T.E., 1998. The effect of fault slip on permeability and permeability anisotropy in quartz gouge. Tectonophysics, 295(1–2): 41–52.
Zhao, M., Zhang, S., and Liao, Z., 2001. The cracking gas from crude oil and its significance in gas exploration. Petroleum Exploration and Development, 28(4): 47–49 (in Chinese with English abstract).
Zhu, G., Fei, A., Zhao, J., and Liu, C., 2014. Sulfur isotopic fractionation and mechanism for Thermochemical Sulfate Reduction genetic H_2S. Acta Petrologica Sinica, 30(12): 3772–3786 (in Chinese with English abstract).

About the first and corresponding author

YUAN Yusong, male, born in 1967 in Hunan Province; doctor; graduated from the Institute of Geology and Geophysics, Chinese Academy of Sciences; professor in Petroleum Exploration and Development Research Institute, SINOPEC. He is mainly engaged in tectonothermal evolution of sedimentary basins and petroleum preservation estimation. E-mail: yuanys.syky@ sinopec.com